Electrons in incommensurate crystals: Spectrum and localization

C. de Lange and T. Janssen
Institute for Theoretical Physics, University of Nijmegen, Toernooiveld 1, 6525-ED Nijmegen, The Netherlands
(Received 8 March 1982)

Electronic properties of incommensurate crystals are studied on a one-dimensional Kronig-Penney model with sinusoidally modulated atomic positions. Spectra and wave functions have been calculated numerically as a function of the modulation wave vector. Information for the incommensurate case is obtained by considering series of commensurate approximants. It is shown that the spectrum of this model has a hierarchical and recursive nature connected with the continued-fraction expansion of the modulation wave vector. In the present model there are parts of the spectrum where the energy eigenvalues occur in bands with a finite number of numerically nonvanishing gaps (bandlike spectrum) and parts where new gaps open up at each step of the continued-fraction expansion (Cantor-type or discrete spectrum). Numerical evidence is presented that the electron states are extended in the bandlike regions and localized in the discrete regions. The characterization of the electron density is made more transparent if one considers the generalized density in (two-dimensional) "superspace." The localized electronic states violate the Fröhlich assumption for the translational freedom of the modulation wave. This has consequences for the electrical conductivity in this model.

I. INTRODUCTION

During the past two decades, incommensurate crystal structures have received a rapid growing attention, both from experimentalists and theoreticians. At present, it has become apparent that in nature there are a great number of systems in which incommensurability plays a role. An example of such systems will be studied in this paper, namely, systems where the atomic equilibrium positions deviate from a regular crystal lattice. In this context, the expression "displacive modulation" is used. Unlike disordered solids, however, these deviations are not random, but systematical. We may represent these deviations by some periodic modulation function superimposed on a regular lattice with a period such that the period of the modulation is incommensurate with the lattice.

A well-understood system of this type is one with a so-called charge density wave (CDW) in quasi-one- or two-dimensional compounds. Peierls[1] and Fröhlich[2] have already shown in the early 1950s that in one-dimensional conductors a spatial modulation of the conduction electron density, with a wave vector which is exactly twice as large as the Fermi wave vector k_F, is energetically favorable. Hence, depending on k_F, it is possible that the CDW is incommensurate with the crystal lattice. The modulation stems from the coupling to the lattice. Therefore, there will be a periodic deformation of the crystal structure. Such an incommensurate periodic modulation of atomic positions has also been observed in insulators, although the origin is not as clear as in the CDW case. There are several other types of incommensurate structures. Moreover, incommensurability is not restricted to crystal structures only (see, for instance, Ref. 3).

From a theoretical point of view, the intrinsic problems of incommensurability are quite intriguing. Many concepts upon which solid-state theory is based, have to be adapted in a nontrivial sense (for example, de Wolff[4] and Janner and Janssen[5] have shown that by introducing space groups in higher dimensions than the usual three, one can restore the lattice periodicity which was lost due to the incommensurate modulation).

The present authors have studied[6] the implications of incommensurability for the phonon spectrum of several one-dimensional models. For this purpose a superstructure approach was used. This method reveals a surprising relation between the structure of the spectrum and the continued-fraction expansion of the ratio of the modulation wavelength and the lattice period. This method was originally used by Hofstadter for a similar model.[7] The physical background of his model is quite different, though. Hofstadter was concerned with the problem of a quantum particle that experiences simultane-

ously a periodic electric and a homogeneous magnetic field. By chance, Hofstadter's simple model gives rise to the same equations as a tight-binding model that represents an electron in an incommensurate crystal. In this paper we will be concerned with the latter problem. There are several reasons to study electrons in incommensurate structures. As we have mentioned previously, they play a role in the origin of the incommensurate phase in certain compounds (CDW). On the other hand, their properties will be different from those in ordinary crystals, just as there is a difference between electrons in disordered systems and in crystals. The behavior of electrons in amorphous materials is governed by the intrinsic randomness, whereas there is a perfect long-range order in an incommensurate crystal. To study the spectrum and nature of electron states in incommensurate crystals we will use the same methods with some minor adaptations which we have used for the phonon model.

II. ELECTRONS IN INCOMMENSURATE CRYSTAL STRUCTURES

As one has seen recently, the character and the spectrum of lattice vibrations in incommensurate crystal phases are in some respects quite different from those of an ordinary crystal.[6,8–10] This is due to the lack of lattice translational symmetry. One can expect similar differences for the behavior of electrons. One way to study electron bands in incommensurate phases is by the use of a tight-binding approximation which is essentially a one-band approximation and especially appropriate for bound electrons. As a matter of fact, the tight-binding approximation for electrons in one dimension is closely related to a one-dimensional model for lattice vibrations. In the context of incommensurability this relation has been discussed by Aubry,[8] by Sokoloff,[9] and by Janssen and Janner.[11] Several results for the phonon problem carry over to the electron problem.

A second way to study electrons in incommensurate crystals is to consider an electron in a quasiperiodic potential. For an incommensurate crystal such a quasiperiodic potential is of the form

$$V(\vec{r})=\sum_{\vec{q}\in M^*} V(\vec{q})e^{i\vec{q}\cdot\vec{r}} . \tag{1}$$

Here M^* is the set of vectors

$$\vec{q}=\sum_{i=1}^{3+d} h_i \vec{a}_i^* , \tag{2}$$

where the vectors $\vec{a}_{3+j}^*$ $(j=1,\ldots,d)$ are incommensurate with respect to a three-dimensional basis $\vec{a}_1^*,\vec{a}_2^*,\vec{a}_3^*$ which is in an incommensurate crystal structure the reciprocal basis of the so-called basic structure. A number of results, of a mathematical nature, for the eigenvalue problem with a potential of the form (1) have been obtained by Dinaburg and Sinai,[12] but, in view of the augmented knowledge of incommensurate phases, it is worthwhile to reconsider this problem.

After this paper had been submitted for publication we saw that quite recently there has been renewed interest in the problem from mathematicians and mathematical physicists.[13–22] Especially for a tight-binding model new results have been obtained. A review of these new developments has been given by Simon.[13]

The origin of the difficulty of the problem lies in the fact that $V(\vec{r})$ does not have lattice periodicity. As has been shown, however, by de Wolff[4] and Janner and Janssen,[5] the symmetry group is a crystallographic space group in $3+d$ dimensions. The potential $V(\vec{r})$ is then the restriction to three-dimensional space of a function V in the $(3+d)$-dimensional space. We here restrict ourselves to the case of a one-dimensional modulation ($d=1$) which is not an essential restriction, though. One considers in a four-dimensional space a lattice Σ^* with basis,

$$\begin{aligned} a_i^* &= (\vec{a}_i^*,0), \quad i=1,2,3 \\ a_4^* &= (\vec{a}_4^*,1) \end{aligned} \tag{3}$$

which is the reciprocal of a basis of a lattice Σ,

$$\begin{aligned} a_i &= (\vec{a}_i,-\vec{a}_4^*\cdot\vec{a}_i), \quad i=1,2,3 \\ a_4 &= (0,2\pi) . \end{aligned} \tag{4}$$

For an incommensurate crystal there is a one-to-one correspondence between the points of the lattice Σ^* and those of the set M^* in three dimensions. Hence, if the four-vector $k=(\vec{k},k_I)$ corresponds to the three-vector $\vec{k}$, the function

$$V(\vec{r},t)=\sum_{\vec{q}\in M^*} V(\vec{q})e^{i(\vec{q}\cdot\vec{r}+q_I t)} \tag{5}$$

is a well-defined function in four-space. Moreover, it has translational symmetry Σ and $V(\vec{r})$ is obtained from $V(\vec{r},t)$ by setting t equal to zero, where t can be interpreted as the phase of the modulation.

If one considers t as a parameter, the Schrödinger equation becomes

$$\begin{aligned} H(t)\psi(\vec{r},t) &= \left[\frac{p^2}{2m}+V(\vec{r},t)\right]\psi(\vec{r},t) \\ &= E(t)\psi(\vec{r},t) . \end{aligned} \tag{6}$$

Here $\vec{p}$ is the usual differential operator, acting only on the variable $\vec{r}$. Because of the lattice symmetry,

the equations and the spectra for t and

$$t+2\pi m-\sum_{i=1}^{3} n_i \vec{a}_4^* \cdot \vec{a}_i$$

are the same. Consequently, one may put

$$E(t)=E(t+2\pi m-\sum_{i=1}^{3} n_i \vec{a}_4^* \cdot \vec{a}_i) ,$$

$$\text{integers } m,n_1,n_2,n_3 . \quad (7)$$

For incommensurate crystals the values of the argument on the right-hand side are dense and E becomes independent of t.

Owing to the lattice symmetry Σ of the Schrödinger equation (6), the eigenfunctions $\psi(\vec{r},t)$ have the Bloch property. They are of the form

$$\psi(\vec{r},t)=e^{i(\vec{k}\cdot\vec{r}+k_I t)} U(\vec{r},t) , \quad (8)$$

where $U(\vec{r},t)$ has the lattice symmetry Σ. If one does not consider t as a dynamical variable, as we have done by writing the Schrödinger equation with t as a parameter, the relative phase of solutions for various values of t is irrelevant and we may put $k_I=0$. This is in agreement with the labeling of phonons in incommensurate crystals,[23] but this assumption may be unjustified if t is a dynamical variable, e.g., if one takes into account the interaction between phonons and electrons.

The Schrödinger equation is reduced to an equation for the function $U(\vec{r},t)$, which is determined by its value in a unit cell of Σ via

$$U(\vec{r},t)=U\left[\vec{r}-\sum_{i=1}^{3} n_i \vec{a}_i, t+\sum_{i=1}^{3} n_i \vec{a}_4^* \cdot \vec{a}_i + 2\pi m\right] . \quad (9)$$

This equation, however, is not an equation for a single value of t: As one sees from Eq. (9) an infinite number of values $0<t<2\pi$ are coupled.

The eigenfunctions transform according to irreducible representations of the symmetry group, which is a four-dimensional space group. Hence, the functions $U(\vec{r},t)$ are labeled by a wave vector $\vec{k}$ and a label for the little group representation for this $\vec{k}$ (the band index). Therefore, the higher-dimensional symmetry group may be of relevance: In the "superspace group" rotations and reflections may be present, which do not exist in the symmetry group of the three-dimensional structure (which is not a three-dimensional space group). The effect of the translational symmetry is to reduce the problem from an infinite unit cell in three dimensions to a finite unit cell (in one dimension more, though).

For an ordinary perfect crystal, all eigenstates are extended, i.e., the wave functions remain finite also for $|\vec{r}|\to\infty$. The same is true for incommensurate crystals provided $U(\vec{r},t)$ is a smooth function. Taking $t=0$ in Eq. (9) and choosing m,n_1,n_2,n_3 in such a way that the argument of the right-hand side is in the unit cell, one sees that if $\psi(\vec{r},0)$ goes exponentially to zero for $|\vec{r}|\to\infty$, the function $U(\vec{r},t)$ has a dense set of zeros. This means that in order to have localized states, $U(\vec{r},t)$ should be nonanalytic. The connection between localization and nonanalyticity has also been discussed, in another context, by Aubry.[8]

The construction of the potential $V(\vec{r},t)$ is only unique if $\vec{a}_4^*$ is incommensurate. However, by continuity one can define V also for commensurate values. Actually, the superspace approach is justified because it does not depend on the exact value of $\vec{a}_4^*$. On the other hand, one may approximate an irrational value of the components by a rational one (with large denominator). Then the potential is periodic (in general with large period) and describes a superstructure. In the sequel we shall try to get information for incommensurate crystals by using such a superstructure approach. For commensurate $\vec{a}_4^*$ the eigenvalues E depend on t. In this case, again the solution for t is only coupled to solutions for $t+2\pi m+\sum_{i=1}^{3} n_i \vec{a}_4^* \cdot \vec{a}_i$ (for all $m,n_i \in Z$). The number of t values in this set is exactly the length N of the unit cell of the three-dimensional superstructure. Again the Schrödinger equation reduces to an equation for $U(\vec{r},t)$, where t is now restricted to the N values coupled by translations. To solve the full problem one has to solve the Schrödinger equations for all values $0\le t<2\pi/N$, separately.

III. THE MODULATED KRONIG-PENNEY MODEL

The character of the eigenfunctions and the spectrum can be studied on a particular one-dimensional example for V. We choose here a modified Kronig-Penney model: The potential $V(x,t)$ is given by

$$V(x,t)=\sum_{n=-\infty}^{\infty} \gamma\delta(x-x(n,t)) , \quad (10)$$

which corresponds to a set of δ-function potentials on the sites of a displacively modulated crystal. This model has also been studied by Azbel in a quasiclassical approximation.[24] The atomic positions are given by

$$x(n,t)=na+u(qn+t) , \quad (11)$$

where u is a periodic function with wave vector q and phase t. Because of the periodicity of the modulation function and $k_I=0$, it holds that

$$\psi(x,t+2\pi)=\psi(x,t) . \tag{12}$$

The potential $V(x,t)$ is invariant under the simultaneous replacements of x by $x+a$ and t by $t-q$. Therefore, the Bloch condition takes the form

$$\psi(x+a,t-q)=e^{ika}\psi(x,t) . \tag{13}$$

Between the nth and $(n+1)$th potential barrier, the wave function can be written as

$$\psi(x,t)=A_n(t)e^{i\alpha x}+B_n(t)e^{-i\alpha x} ,$$
$$x(n,t)<x<x(n+1,t) \tag{14}$$

where $\alpha^2=(2m/\hbar^2)E$.

Owing to the Bloch condition (13), the amplitudes $A_n(t)$ and $B_n(t)$ of the nth and $(n+1)$th cell are related

$$A_n(t)=e^{-i(k-\alpha)a}A_{n+1}(t-q) ,$$
$$B_n(t)=e^{-i(k+\alpha)a}B_{n+1}(t-q) . \tag{15}$$

As usual, the next step is to match the wave function ψ and its derivative $d\psi/dx$ across a barrier, say at $x=x(n+1,t)$. This yields

$$\begin{bmatrix} A(t) \\ B(t) \end{bmatrix} = e^{ika}T \begin{bmatrix} A(t+q) \\ B(t+q) \end{bmatrix} . \tag{16}$$

First we note that the index n has been dropped in this equation. Owing to the recurrent nature of Eq. (15), it is sufficient to obtain information of only one of the A_n's and B_n's, say for $n=0$. All the other coefficients are given by Eq. (15). Therefore, we define as a shorthand notation: $A(t)=A_0(t)$ and $x(t)=x(1,t)$.

The matrix T of Eq. (16) that transfers information of the coefficients $A(t+q)$ and $B(t+q)$ to the coefficients $A(t)$ and $B(t)$ is given by

$$T=\begin{bmatrix} e^{-i\alpha a}\left[1+\frac{ig}{2\alpha}\right] & e^{i\alpha a}\left[\frac{ig}{2\alpha}\right]e^{-2i\alpha x(t)} \\ e^{-i\alpha a}\left[\frac{ig}{2\alpha}\right]e^{2i\alpha x(t)} & e^{i\alpha a}\left[1-\frac{ig}{2\alpha}\right] \end{bmatrix} , \tag{17}$$

where $g=2m\gamma/\hbar^2$.

It is easy to obtain a recurrence relation between the coefficients A only. For this purpose, we replace t by $t-q$ in the first of the two relations defined by Eq. (16) giving a relation between $A(t-q)$, $A(t)$, and $B(t)$. A second relation, now between $A(t+q)$, $A(t)$, and $B(t)$ is easily obtained by inversion of matrix Eq. (15), because $\det T=1$. Combining these two relations to eliminate $B(t)$, we get

$$e^{-i[ka-\alpha f(t)]}A(t-q)+e^{i[ka-\alpha f(t)]}A(t+q)=\{2\cos[\alpha(a-f(t))]+\frac{g}{\alpha}\sin[\alpha(a-f(t))]\}A(t) , \tag{18}$$

where $f(t)=x(t-q)-x(t)$.

Provided that the wave vector q of the modulation function satisfies the rationality condition

$$q=2\pi\frac{L}{N} , \tag{19}$$

the band structure of the energy spectrum can be calculated. In this case the condition for α can be written as a secular determinant equation

$$\det\begin{bmatrix} a_0 & b_0e^{ika} & \cdots & & b_0^*e^{-ika} \\ b_1^*e^{-ika} & a_1 & b_1e^{ika} & & \vdots \\ & b_2^*e^{-ika} & a_2 & b_2e^{ika} & \\ & & \ddots & \ddots & \\ b_{N-1}e^{ika} & \cdots & & b_{N-1}^*e^{-ika} & a_{N-1} \end{bmatrix}=0 , \tag{20}$$

where

$$a_l=2\cos[\alpha((a-f(t+lq))]+(g/\alpha)\sin[\alpha(a-f(t+lq))]$$

and $b_l=-\exp[-i\alpha f(t+lq)]$. The dependence on k for this kind of equation can be given explicitly

$$\det\begin{bmatrix} a_0 & b_0 & \cdots & & b_0^* \\ b_1^* & a_1 & b_1 & & \vdots \\ & b_2^* & a_2 & b_2 & \\ & & \ddots & \ddots & \\ b_{N-1} & \cdots & & b_{N-1}^* & a_{N-1} \end{bmatrix} = b_0 b_1 \cdots b_{N-1}(e^{ikNa}-1)+b_0^* b_1^* \cdots b_{N-1}^*(e^{-ikNa}-1)$$

$$=2\cos(Nka)-2 , \tag{21}$$

where use has been made of the fact, that

$$\sum_{l=0}^{N-1} f(t+lq)=\sum_{l=0}^{N-1} x(t+(l-1)q) - x(t+lq)=0 . \tag{22}$$

The band structure can now be determined in exactly the same way as for an unmodulated crystal. In the latter case the determinant of Eq. (19) reduces to the well-known condition of Kronig and Penney for the allowed values of α

$$2\cos(\alpha a)+g/\alpha \sin(\alpha a)=2\cos(ka) . \tag{23}$$

The left-hand side of this equation has to lie between $+2$ and -2 (this is illustrated, for instance, in Fig. 4.2 of Ref. 25). If the atomic positions are modulated, Eq. (19) gives the condition for the bands in this case. Similarly, the determinant has to lie between -4 and 0. For a given modulation function, we can calculate the determinant as a function of α by means of a computer. The problem reduces to a search for those values of α for which the determinant equals -4 and 0. As an example, we calculated band structures for the case in which the atomic positions are simply given by

$$x(n,t)=na-\Delta a\cos(qn+t) , \tag{24}$$

and we chose the following values for the various dimensionless parameters

$$ga=\frac{3\pi}{2}, \quad \frac{\Delta a}{a}=10^{-1/2}, \quad t=0 . \tag{25}$$

In Fig. 1 the results have been put in a graph. The spectra that are displayed are those for $N=50$ and $L=0,1,2,\ldots,50$. Professor J. Avron showed us a similar graph for the same model with slightly different values of the parameters, which agrees very well with our results.

IV. RECURSIVE NATURE OF THE MODULATED KRONIG-PENNEY SPECTRUM

Both Azbel[26] and Hofstadter[7] have shown that the spectrum of the tight-binding model has a hierarchical and recursive nature, i.e., the spectrum splits into clusters of bands, which in turn split into subclusters, whereupon they split into sub-subclusters, and this splitting continues *ad infinitum*, when the modulation wave vector is incommensurate, whereas in the commensurate case, i.e., for $q/2\pi=L/N$ (L and N relatively prime), the final splitting is N-fold. For a given value of q, the splitting is strongly related to the continued-fraction expansion of $q/2\pi$. This continued-fraction expansion can be written in the standard way

$$\frac{q}{2\pi}=a_0+\cfrac{1}{a_1+p_1/q_1} = a_0+\cfrac{1}{a_1+\cfrac{1}{a_2+p_2/q_2}} = a_0+\cfrac{1}{a_1+\cfrac{1}{a_2+\cfrac{1}{a_3+\cdots}}} , \tag{26}$$

where a_i, p_i, and q_i are integers (note that, in general, $p_{i-1}=q_i$).

Using a WKB method, Azbel anticipated that the spectrum consists of a_1 clusters of bands, each of which splits into a_2 subclusters, each of which splits into a_3 sub-subclusters, and so on. Owing to the nature of the WKB method, this only holds for large values of the a_i's (recently Sokoloff has shown how Azbel's approach can be extended to smaller values of the a_i's).[27] Azbel's results agree well with the exact calculations of Hofstadter for rational values of $q/2\pi$. For smaller values of the a_i's, Hofstadter's calculations show, after inspection of a large number of spectra, that the clustering patterns are somewhat more complicated.

This rather simple connection between the cluster pattern for given q and its continued-fraction expansion is due to the fact that the modulation function that we consider has only one Fourier component, as was shown in Refs. 6 and 28. When there are more Fourier components involved, the splitting gets more complicated. Similar models, such as the Frenkel-Kontorova model, exhibit exactly the same behavior, although the formula according to which

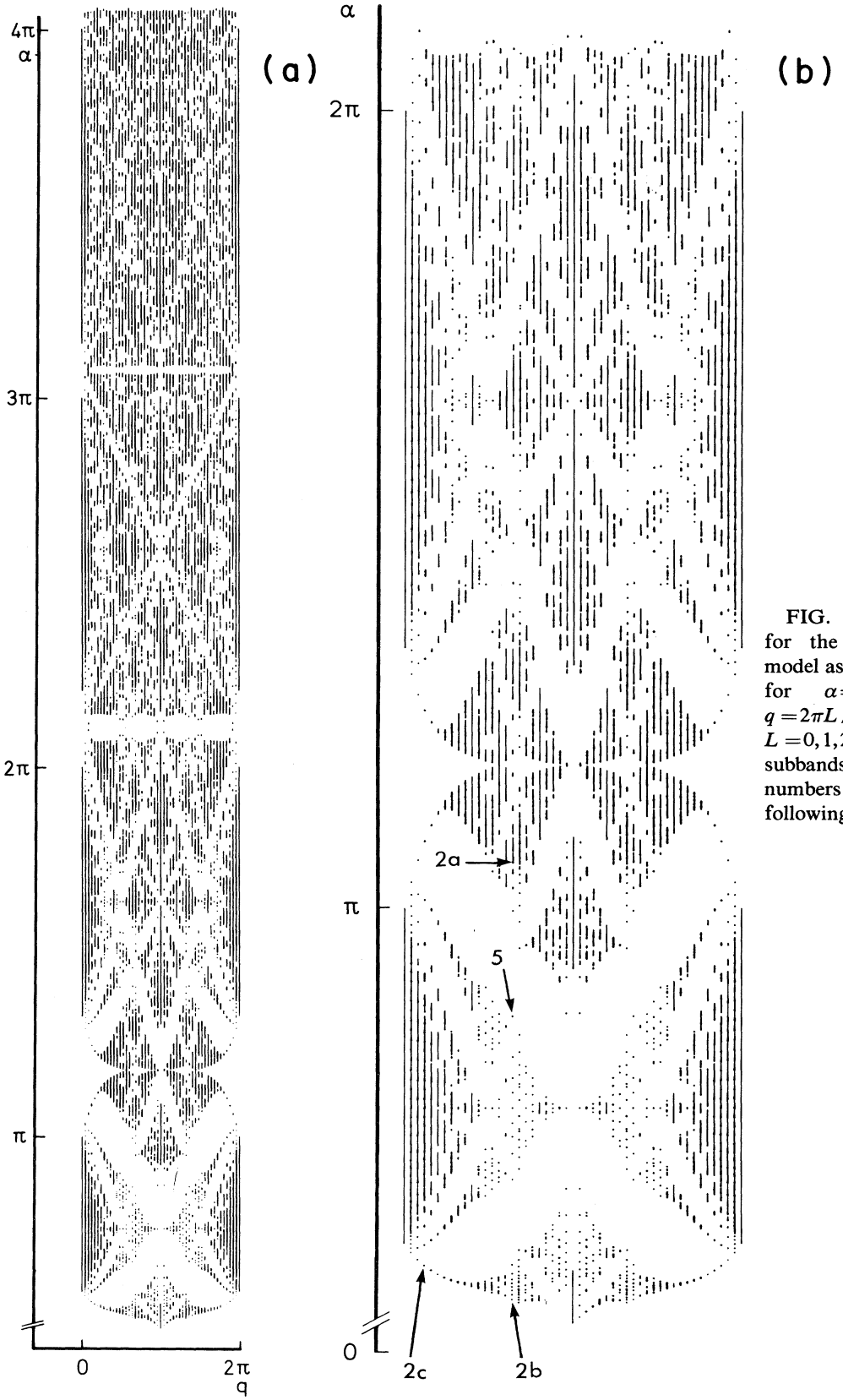

FIG. 1. (a) Lowest $4N$ subbands for the modulated Kronig-Penney model as a function of q. The spectra for $\alpha=(2m/\hbar^2)E$ plotted for $q=2\pi L/N$ with $N=50$ and $L=0,1,2,\ldots,50$. (b) The lowest $2N$ subbands of (a) are enlarged. The numbers in this picture refer to the following figures.

the bands cluster is slightly different for the various models.

The question arises to what extent the modulated Kronig-Penney model exhibits similar features. At first sight this system appears to be more troublesome. Unlike the models which we mentioned above and which are essentially phonon models or one-band models in the electron context, the Kronig-Penney model has no limitation to a maximum energy, i.e., the unperturbed Kronig-Penney model has an infinite number of bands. It turns out that when the modulation of the atomic positions is "switched on," each of the original bands breaks up in exactly N subbands, if the modulation function repeats itself after N atoms. This agrees with the general analysis in Ref. 25 for Hill's equation (the Kronig-Penney model is a special case of this equation). In this context it may be important, as Toda's analysis shows, that it is possible that the width of some gaps vanishes. As one can see in Fig. 1 there are regions where the gaps become extremely narrow. We call the spectrum there "bandlike." On the other hand, there are also regions where the spectrum consists of very narrow bands separated by relatively large gaps. Here we use the term discrete or Cantor-type spectrum. As an illustration a number of bands are given in Table I for two typical cases: a bandlike region for $L/N=\frac{1}{50}$, where the gaps are smaller than 10^{-7}, and a Cantor-type region for $L/N=\frac{8}{25}$, where the bands form only 4 per thousand of the whole interval. Although it has been conjectured that for almost every incommensurate potential the spectrum is a Cantor set, in the present model there are gaps which are either zero or so small that from a physical point of view they may be neglected.

If we study the graph of Fig. 1 more carefully, it appears that the lower part of the graph exhibits the most visible structure; for higher energies the structure gets rather messy. It turns out, much to our surprise, that the lowest N subbands for a given value of q $(=2\pi L/N)$ have the same clustering pattern as the total spectrum of the tight-binding model. For this model Hofstadter has formulated a general formula that gives the clustering pattern for arbitrary q. For the sake of convenience we will repeat the description of this formula briefly in this paper.

Let $\Pi(\beta)$ denote the clustering pattern for $\beta=q/2\pi$. So, for example, $\Pi(2/5)=2\text{-}1\text{-}2$ means a cluster of five bands with the lowest and highest pairs close together. The breaking up of the spectrum into clusters for a given value of β can be represented by

$$\Pi(\beta)=\Pi(\beta')\Pi(\alpha')\Pi(\beta') . \tag{27}$$

When N is the largest integer less than or equal to $1/\beta$, the relations between β' and β, and α' and β are given by

$$\beta=(N+\beta')^{-1},\quad \beta=\left[2+\frac{1}{\alpha'}\right]^{-1},\quad 0<\beta\leq\tfrac{1}{2} . \tag{28}$$

If $\frac{1}{2}<\beta<1$, one can simply replace β by $1-\beta$. More details are found in Ref. 7.

In Ref. 7 an example was given for the decomposition of the spectrum for $\beta=\frac{5}{17}$. Hofstadter's analysis shows that $\Pi(\frac{5}{17})$ is given by

$$\Pi(\tfrac{5}{17})=\Pi(\tfrac{2}{5})\Pi(\tfrac{5}{7})\Pi(\tfrac{2}{5}) .$$

The decomposition can be carried on another step by

TABLE I. Ten bands from the spectra for two values of L/N. For $L/N=\frac{1}{50}$ a bandlike part of the spectrum with (numerically) vanishing gaps, for $L/N=\frac{8}{25}$ a Cantor-type part with nearly discrete levels (cf. Fig. 1).

$\frac{L}{N}=\frac{1}{50}$			$\frac{L}{N}=\frac{8}{25}$			
E_{bottom}	E_{top}	Gap	E_{bottom}	E_{top}	Width	Gap
1.963 759 4	1.986 291 9	9×10^{-7}	1.600 825 3	1.600 829 1	38×10^{-7}	0.0198
1.986 292 8	2.010 382 7	0	1.620 622 6	1.620 679 9	573×10^{-7}	0.0166
2.010 382 7	2.035 945 9	0	1.637 328 1	1.637 641 9	3138×10^{-7}	0.0131
2.035 945 9	2.062 906 3	0	1.650 753 0	1.651 453 0	7000×10^{-7}	0.0130
2.062 906 3	2.091 185 6	0	1.664 549 8	1.665 304 2	7544×10^{-7}	0.0151
2.091 185 6	2.120 710 4	0	1.680 439 9	1.680 839 5	3996×10^{-7}	0.0221
2.120 710 4	2.151 408 2	0	1.702 934 3	1.703 026 8	925×10^{-7}	0.0353
2.151 408 2	2.183 206 6	0	1.738 277 4	1.738 286 0	86×10^{-7}	0.3373
2.183 206 6	2.216 033 0	0	2.075 560 6	2.075 561 5	9×10^{-7}	0.1023
2.216 033 0	2.249 816 9	0	2.177 903 2	2.177 916 5	133×10^{-7}	0.0869

noting that

$$\Pi(\tfrac{2}{5})=\Pi(\tfrac{1}{2})\Pi(0)\Pi(\tfrac{1}{2}) ,$$

$$\Pi(\tfrac{5}{7})=\Pi(\tfrac{1}{2})\Pi(\tfrac{1}{3})\Pi(\tfrac{1}{2}) .$$

The picture of Ref. 7 demonstrating this clustering can now be compared with the spectrum of the Kronig-Penney model for the same value $\frac{5}{17}$ of β. In Table II the lowest 51 subbands of the Kronig-Penney model are given for this value of β. Although the cluster patterns for Hofstadter's tight-binding and for the lowest N subbands of the Kronig-Penney model are exactly the same for the corresponding modulation wave vector q, this does not hold for the subbands themselves. One of the pronounced differences between the two models is the tendency of the subbands to broaden as the energy increases in the case of the Kronig-Penney model. This does not happen for the Hofstadter model, where the spectrum possesses a mirror symmetry through which the widths of the lower and upper subbands are equal. This is certainly not the case for the Kronig-Penney model. In this respect it is remarkable, though, that the Kronig-Penney spectrum does exhibit mirror symmetry in the vicinity of those gaps that remain if the modulation is "switched off" (i.e., the gaps near π, 2π, etc., in Fig. 1).

For the next group of N subbands of the Kronig-Penney model, it is already more complicated to formulate a cluster pattern formula, and the structure gets even more complex for higher energies. We did not attempt to formulate the cluster pattern for higher energies, although in all cases that we studied the spectrum kept breaking up in clusters with a number of subbands, which corresponds to the last stages of the continued-fraction expansion of $q/2\pi$ (see, for example, the last columns in Table II).

V. NATURE OF THE ELECTRONIC STATES

In the preceding section we discussed the relation between the cluster pattern of the spectrum and the continued-fraction expansion of the modulation wave vector. However, the spectrum has another

TABLE II. Illustration of the decomposition into subclusters, sub-subclusters, etc., of the lowest 51 subbands for $q/2\pi=L/N=\frac{5}{17}$. Only the cluster patterns of the first N subbands are indicated. For higher subbands the structure is still present but less obvious as one sees easily. Note that the continued-fraction expansion of $\frac{5}{17}$ stops after two stages. This table can directly be compared with Table 1 of Ref. 6.

First N subbands		Cluster pattern		Second N subbands		Third N subbands	
Bottom	Top	First stage	Second stage	Bottom	Top	Bottom	Top
1.6204	1.6213			3.7154	3.8223	6.7261	6.7708
1.6270	1.6284		2	3.8327	3.8998	6.8122	6.8546
1.6561	1.6576	$\Pi(\frac{2}{5})$	1	4.0620	4.0971	7.0915	7.1145
1.6824	1.6845		2	4.1955	4.2418	7.2915	7.3522
1.6963	1.6974			4.2869	4.3164	7.3861	7.4571
2.0800	2.0805			4.6153	4.6478	7.6164	7.7028
2.1046	2.1053		2	4.6497	4.6809	7.7260	7.8463
2.2810	2.2820			5.0558	5.0992	7.8829	7.9706
2.3553	2.3571	$\Pi(\frac{5}{7})$	3	5.1000	5.1832	8.1066	8.1648
2.4334	2.4346			5.1888	5.2350	8.3084	8.4035
2.6678	2.6693		2	5.5735	5.6211	8.4225	8.5481
2.7031	2.7058			5.6395	5.7262	8.5827	8.6664
3.2320	3.2447			5.7765	5.8658	8.8356	8.8959
3.2718	3.2990		2	5.9003	5.9617	8.9872	9.0471
3.3687	3.3965	$\Pi(\frac{2}{5})$	1	6.1115	6.1344	9.2186	9.2897
3.5259	3.5877		2	6.3891	6.4274	9.3602	9.4627
3.5991	3.7021			6.4721	6.5141	9.5207	9.6275

striking feature which will turn out to have important implications for the nature of the eigenstates. When we take a look at the spectrum, in particular to the lower part, for an arbitrary value of q, it is possible to distinguish between regions where the allowed energies look like discrete levels and other regions where they look like bands.

For phonon models similar to the tight-binding model we mentioned before, we have shown in Ref. 6 that the energy spectrum changes its character at a limiting value of the amplitude of the modulation function. As Hofstadter made plausible, at the transition value the spectrum becomes a Cantor set for incommensurate wave vectors; the spectrum consists of an infinite set of discrete energy levels. When the amplitude gets smaller, though, the gaps in the density of states corresponding to each stage of the continued-fraction expansion diminish with each successive step, so that ultimately they tend to zero (see also Ref. 29). Thus, even though for incommensurate modulation wave vectors the decomposition process keeps on forever, there remain bands, some of them separated by relatively large gaps, corresponding to the first stages of the continued-fraction expansion.

Aubry has pointed out that the transition value of the modulation amplitude for the tight-binding model also corresponds to a transition from a situation where all eigenstates are extended, to a situation where they all are localized. In this respect the Kronig-Penney model might be a little more interesting than the tight-binding model. Both bands and discrete levels occur within the same spectrum, at least for the values of the parameters that have been studied in this paper. This could mean that extended and localized states occur simultaneously as was predicted by Azbel.[24] For this reason we examined the wave functions corresponding to different energy regions. In particular, we paid attention to any difference between states corresponding to discrete levels and those belonging to bands. A similar investigation for the disordered Kronig-Penney model was performed by Borland.[30]

We simply calculate for a given strength of the δ potentials γ, the Bloch wave vector k corresponding to a certain energy within a subband, and then we determine the corresponding coefficients $A(t+nq)$ and $B(t+nq)$, for $n=0,\ldots,N-1$. Expressed in $A(t+nq)$ and $B(t+nq)$ and complex conjugates, the probability density reads

$$|\psi(x)|^2=A^*(t+nq)A(t+nq)+B^*(t+nq)B(t+nq)+A^*(t+nq)B(t+nq)e^{-2i\alpha(x-na)}$$
$$+B^*(t+nq)A(t+nq)e^{2i\alpha(x-na)},\quad x(n,t)<x<x(n+1,t)\ . \tag{29}$$

To get an indication of what the wave functions look like in an incommensurate case, we compared several eigenstates corresponding to commensurate values of the modulation wave vector, lying close to each other. In this respect, it is convenient to compare the results after keeping successive terms in the continued-fraction expansion of an irrational number. As an example, $\frac{8}{25}$, $\frac{17}{53}$, $\frac{42}{131}$ can be thought of as successive approximants of the irrational number for which the beginning of the continued-fraction expansion reads $1/(3+1/\{8+1/[2+1/(2+\cdots)]\})$.

We found a striking difference in the nature of electronic states corresponding to bands and that of states corresponding to discrete levels. Three types of states can be distinguished for incommensurate modulation wave vectors:

(i) Extended states corresponding to broad bands. In this case the "bands" are studded with tiny gaps that correspond to advanced stages of the continued-fraction expansion. However, due to Zener breakdown, these gaps are negligible.[31]

(ii) Localized states corresponding to discrete energy levels. The higher-order gaps remain significant in this case. This situation is similar to the outcome of the construction of a Cantor set, for which the total measure of gaps equals one.[32]

(iii) States which are intermediate between localized and extended. In this case the probability density is periodic but concentrated on equidistant intervals which are separated by intervals where the density practically vanishes. These states occur for very narrow bands, which look like the discrete levels of (ii), but in contrast with (ii) these bands are separated by extremely small gaps instead of large gaps, when they are viewed in detail.

Type (iii) is intermediate in the sense that, if the intervals where the density nearly vanishes become smaller and smaller, this type goes continuously to type (i), whereas type (ii) is approximated if the length of these intervals grows to infinity. To illustrate states of type (i), we displayed in Fig. 2(a) the electron density $|\psi(x)|^2$ as a function of position x, for the series of approximants we mentioned above and for an energy that lies inside a band, which is not extremely narrow. In all three cases the energy was taken to be the same. It should be noted in all cases, we have checked that the electron density as a function of position hardly depends on the Bloch wave vector k; that is to say, as long as we remain

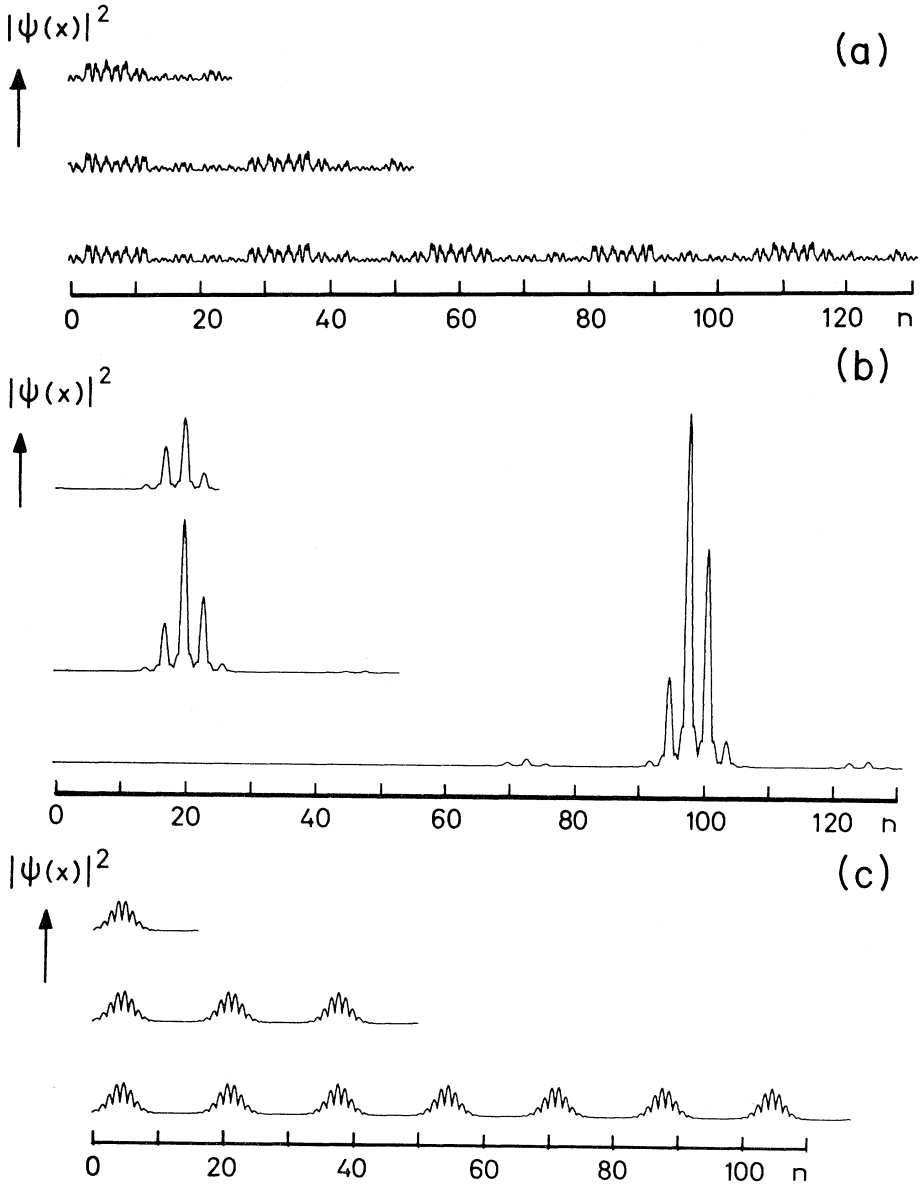

FIG. 2. Three types of electron densities, each for three approximants to an incommensurate modulation wave vector and almost the same energy. In every graph the electron density over one unit cell is plotted. (a) Densities for a rather broad band. The series of approximants is $q/2\pi = \frac{8}{25}, \frac{17}{53}, \frac{42}{131}$. The energy for $\frac{8}{25}$ is indicated in Fig. 1. The wave functions are extended. (b) Densities for an extremely narrow band. The series of approximants is the same as in (a), the energy for $q/2\pi = \frac{8}{25}$ is indicated in Fig. 1. The electron is restricted to a narrow region in the unit cell in each case. In the incommensurate limit the electron will be localized. (c) Densities for an energy where the spectrum has very narrow bands separated by gaps which are three orders of magnitudes smaller. The series of approximants is $\frac{1}{16}, \frac{3}{50}, \frac{7}{117}$. The energy for $\frac{3}{50}$ is indicated in Fig. 1. The electron density is periodic. The pattern is in each case a repetition of that for $\frac{1}{16}$. Between the regions where the electron density is concentrated, the density drops to practically zero.

within one subband.

If one compares the graphs for different q, it appears that the electron density over one supercell in the case where $q/2\pi = \frac{8}{25}$ (the supercell consists of 25 atoms in this case), is repeated twice in a very good approximation for the case where $q/2\pi = \frac{17}{53}$, and this basic pattern is reproduced nearly five times for $q/2\pi = \frac{42}{131}$. The reproduction is even

better when the patterns of $q/2\pi=\frac{17}{53}$ and $\frac{42}{131}$ are compared mutually. All three wave vectors considered here are commensurate. Thus the total picture of the electron density for $-\infty<x<\infty$ in each case is an infinite repetition of the pictures that are plotted in Fig. 2(a). Hence it seems fair to suppose that for an incommensurate modulation wave vector the picture of the electron density will look very much the same, except that the basic pattern will change gradually along the chain. A state for which the electron density is not limited to a certain region of space, or in other words, for which there is finite probability everywhere in the lattice to find the electron, is called "extended." Clearly, the state that we described above falls within this class.

The behavior of the electron density for discrete energy levels is completely different. In Fig. 2(b) we have plotted the electron density for the same series of q values, but for the lowest subband, which in every case is extremly narrow. It is seen that there is no repetitive pattern whatsoever when the different pictures for the successive approximants are compared. However, the electron density has in all three cases the same basic form (namely, three peaks placed upon pedestals). In all cases, the probability is almost zero within a supercell, except for a few very narrow peaks lying close to each other. It should be noted that the probability is normalized in such a way that its integral over one supercell equals the length of the supercell, so that the graphs for different values of q can be compared directly. For example, the supercell for $q/2\pi=\frac{8}{25}$ fits approximately five times in the supercell for $q/2\pi=\frac{42}{131}$, whereas the height of the peaks is 5 times smaller.

The fact that, however large L and N may be, there always remain a few peaks close to each other limited to only a small region of the supercell, implies that for an incommensurate value of q one ends up with a state that is strictly limited to a narrow part of the total chain. Thus we arrive at the important statement that eigenstates corresponding to discrete energy levels are localized.

In this respect we emphasize that one ought to be very careful in concluding which regions of the spectrum for commensurate modulation wave vectors tend to discrete levels for incommensurate wave vectors. This holds only for those regions of the spectrum which are Cantor-type, i.e., those for which the gaps between the band clusters remain of finite size with every step of the continued-fraction expansion of $q/2\pi$. This fact is stressed because sometimes there may occur a cluster of bands which as a whole looks like a single, very narrow band, whereas in reality it is a couple of bands separated by extremely small gaps (the size of the gaps is typically 2 or 3 orders of magnitude smaller than that of the bands). The eigenstates corresponding to this case are illustrated in Fig. 2(c). Here we have plotted the electron densities within a supercell for an energy lying inside the lowest subband for a different series of approximants (i.e., $q/2\pi=\frac{1}{16},\frac{3}{50},\frac{7}{117}$). For $q/2\pi=\frac{1}{16}$ the electron density within a supercell behaves like that corresponding to $q/2\pi=\frac{8}{25}$ in the discrete-levels case. In a large part of the cell the electron density is almost zero and the electron is limited to a small region of the cell. However, the behavior of the next approximants is completely different. If we compare the graph of the electron density for $q/2\pi=\frac{1}{16}$ and $\frac{3}{50}$, we see the same pattern repeated three times, and for $q/2\pi=\frac{7}{117}$ it is repeated seven times. Although in all cases we are dealing with a very narrow band, the trend when going to incommensurate wave vectors is the same as for the broad bands described earlier in this section. Hence we certainly cannot conclude that, in the incommensurate case, the electron is limited to a particular narrow region in space. This strongly suggests the familiar notion that for an isolated discrete energy level the corresponding wave function is localized, or in another terminology, square integrable, whereas in the opposite case where the set of eigenvalues is everywhere dense, the eigenfunctions are extended.

The fact should be mentioned that there seems to be a direct relation between the width of a band and the minimal value of the electron density in the supercell. We observed, for instance, that the mean electron density can drop to a typical value of 10^{-10} over a fairly large range of the chain (compared to a maximum of about 50), if the bandwidth is very small, in this case of the order of 10^{-7}. As the width of a band grows, e.g., if the bandwidth is 10^{-4}, the local mean probability drops to a minimum of 10^{-7}.

Another interesting phenomenon occurs when we study the behavior of the electron density when the phase of the modulation function is changed. First we note that a change from t to $t+2\pi/N$ only signifies a rigid translation of the lattice as a whole. This does not change the spectrum, and the wave functions are simply shifted. This implies that we only have to examine values of t between, e.g., 0 and $2\pi/N$. The results for the same set of examples as in the beginning of this section are plotted in Fig. 3. From these graphs we see that for extended states the electron density changes only gradually when t is varied. However, this is not true when an eigenstate is localized. If $q=2\pi L/N$, the peaks in the electron density shifts a number of lattice sites, when t changes to $t+2\pi/N$. For an intermediate value of t, there is a sharp transition, for which the peak jumps from one position to the other.

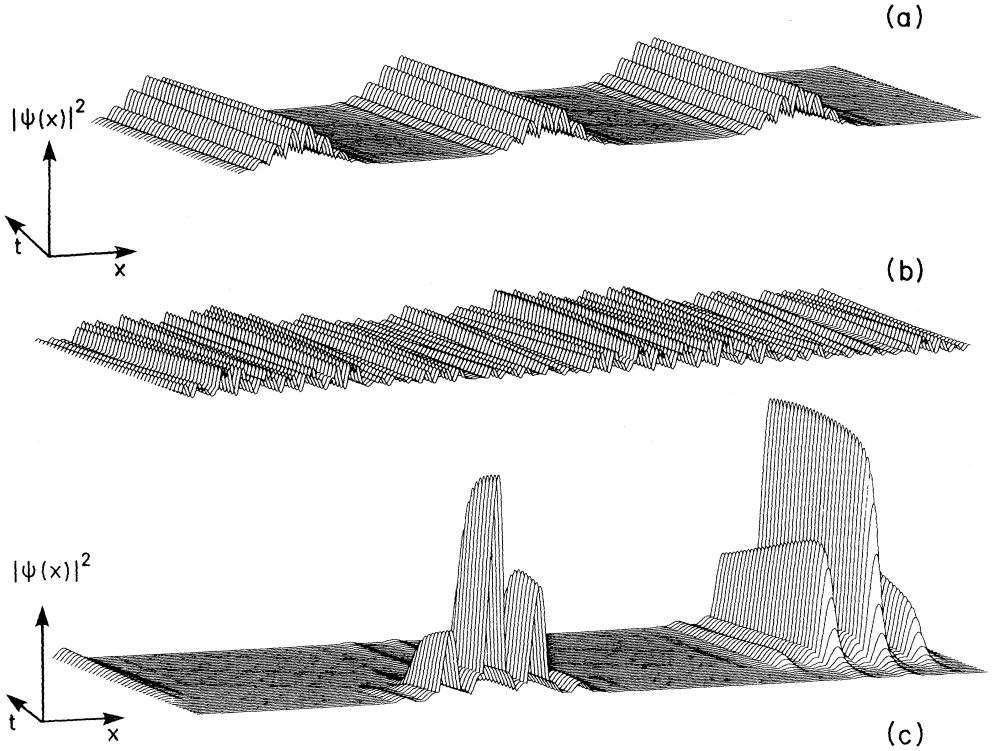

FIG. 3. Electron densities are plotted with the phase t of the modulation function as a parameter, t runs from 0 to $2\pi/N$. The three different cases (a), (b), and (c) correspond with the cases (c), (a), and (b) of Fig. 2, respectively. Each graph corresponds to the middle of each set of three graphs in Fig. 2, i.e., for (b) and (c) $L/N=\frac{17}{53}$ and for (a) $L/N=\frac{3}{50}$. Notice that the peaks in the probability in (c) jump suddenly when t is varied.

At this point we want to remark that the phase t of the modulation function plays the role of the internal coordinate in the superspace group approach of Refs. 4 and 5. Owing to the fact that the Kronig-Penney model and the modulation are both one dimensional, the superspace in our case has two dimensions. The region between two adjacent atoms in the space direction and an interval of 2π in the phase (internal) direction covers the area of a unit cell in superspace. In Fig. 4 we plotted contour lines of the electron density of Fig. 3(c). The parallelogram formed by the centers of the four patterns that are plotted, builds exactly one unit cell. Note that Fig. 4 corresponds to a localized state.

The plot in superspace reveals much more of the structure of the electron density over the range of the whole crystal (i.e., for a fixed value of t) than one would expect at first sight. The picture that emerges from Fig. 4 is that of a narrow island (corresponding to the center peak of Fig. 4) and two satellite islets [corresponding to the side peaks in Fig. 3(c)] separated by steep troughs where the probability drops to almost zero. It is remarkable that the maximum of the density in a unit cell is located at that value of t for which the distance between the atoms is largest. It is seen that there is a great coherence between the shapes of the central and the side peaks. In addition, corresponding plots for $q/2\pi=\frac{8}{25}$ and $\frac{42}{131}$ show that the picture is almost exactly the same in these cases, except for one notable difference, namely, the islands narrow for approximants of increasing order (although they remain centered at roughly the same value of t). The width of an island is $2\pi/N$, so that for an incommensurate modulation wave vector we end up with a couple of equally spaced thin sheets. The spacing depends hardly on the value of q, but it may vary with the specific subband [for instance, the density of Fig. 5 will give another spacing than that of Fig. 2(b)]. When the electron densities for a series of approximants are compared as in Fig. 2(b), this manifests itself as one set of peaks per unit cell (of N atoms) of the superstructure, regardless of the value of N. As we have discussed previously, this fact is

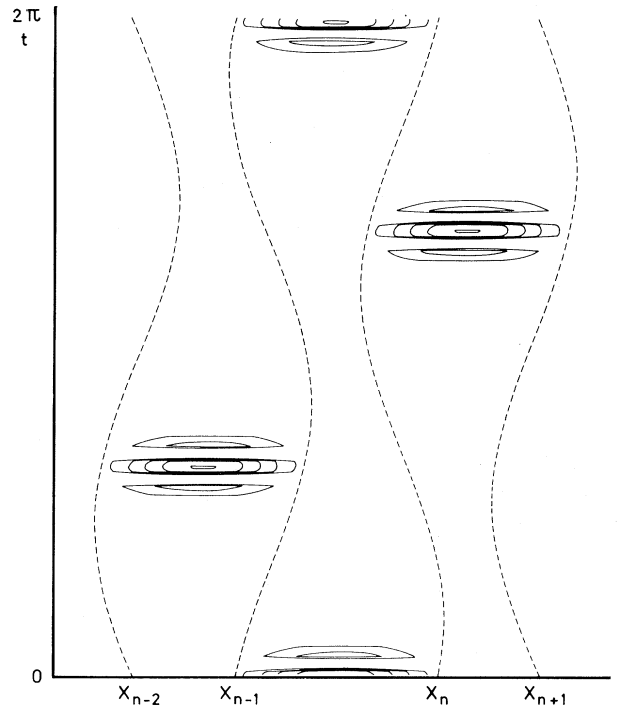

FIG. 4. In superspace the contour lines of Fig. 3(c) are drawn. In a certain sense the scales of the x and t axis are reversed, compared to Fig. 3. In Fig. 3(c) the density was plotted over a range of 53 atoms, in this picture over only 3 atoms, whereas in Fig. 3(c) t ran up to $2\pi/53$ instead of 2π as in the present picture. Note that there are steep troughs between the islands of high density. Otherwise the contour lines of the different islands appear to link up smoothly. This reveals an unexpected structure relating the three peaks in the electron density of Fig. 2(b).

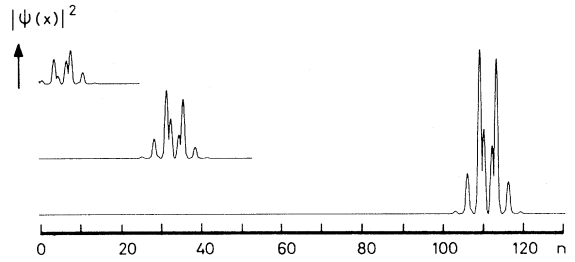

FIG. 5. This figure and Fig. 2(b) are very much alike, except for the part of the spectrum to which they correspond. Figure 2(b) corresponds to the lowest eigenvalues; here the energies are higher (see Fig. 1). The pattern of the three different pictures appears to be closely related.

of great importance because it guarantees the strict localization of the electron state in the incommensurate case. Otherwise, the electron density would exhibit an array of peaks, like the picture of Fig. 2(c).

For nonlocalized states the superspace plot is not so spectacular; it merely consists of smoothly flowing contour lines. For the localized states, however, it yields a great deal of insight. In the first place, it shows in conjunction with plots for other approximants that nothing drastic happens when the modulation wave vector changes slightly, even for incommensurate wave vectors, provided that the character of the subband does not change. This is supported once more by Fig. 5, for which the situation is exactly the same as in Fig. 2(b) except that the electron density corresponds to a higher subband, instead of the lowest. It is seen that the picture for all three approximants is very much the same. The superspace plot reveals an underlying structure that otherwise would have been hidden. It clearly shows that the electron density in different parts of the supercell for a fixed value of the t are related to each other. For example, we could hardly expect beforehand that the shapes of three peaks placed upon pedestals in each graph of Fig. 2(b) are so closely related. The plotted contour lines of the satellite islets appear to join up smoothly with the two outermost ones of the central island. Moreover, it seems that the picture is highly symmetric. If one considers this plot more carefully it appears that the symmetry is violated occasionally. This might be a consequence of the fact that it is not always possible for each single value of t for which we calculated the electron density, to take the same value of the energy, due to dependence of the band function $E(k)$ on t for a commensurate modulation. We did not really study which values of α or k for different t should be related, because the shape of the electron density changes only a few percent over the whole range of k. Owing to this fact, the densities that are related in Figs. 3 and 4 are subject to a certain spread, and this may cause the small deviations from symmetry. These questions should be studied more carefully in the future, the more so because the picture that arises for an actual crystal, which is an intersection of the superspace pattern for a certain value of t, reminds one of the hierarchical and recursive structure that underlies the Kronig-Penney or similar spectra, because the peak pattern is repeated on smaller scales in other parts of the crystal.

Finally, we want to make some remarks on the electrical conductivity of the modulated Kronig-Penney system. According to Fröhlich, an incommensurate phase with the Fermi level at a gap may still be conducting. This happens if the frequency of the coupled electron-phonon mode, which is

described as a shift in phase of the modulation wave, drops to zero. In an incommensurate phase this may occur because of the fact that the energy is independent of the phase, unless the wave function is very discontinuous. However, the superspace plot shows that for localized states the peaks in the electron density jump from one position to another when the phase of the modulation is changed. In other words, the wave function becomes nonanalytic for an incommensurate modulation, preventing the free shift of the modulation phase. Therefore, if the states at the Fermi level are localized, there will be no such Fröhlich mode.

VI. DISCUSSION

With respect to localization properties, incommensurate crystal phases are between ordinary crystals and amorphous materials. The states in an ordinary crystal are all extended; those for a one-dimensional amorphous system are all localized. For an incommensurate crystal the existence of localized states depends on the wave vector of the modulation and on its strength.

If one may draw conclusions for the incommensurate case from results for commensurate approximations, we have found numerical evidence in the displacively modulated Kronig-Penney model for the following situation. The spectrum as function of the modulation wave vector has a hierarchical and recursive structure governed by the continued-fraction expansion of this wave vector. Depending on the latter there are regions in the spectrum which are called bandlike and others which we call Cantor-type. In bandlike regions the measure of the spectrum is nonzero and the gaps go rapidly to zero for successive steps in the continued-fraction expansion. In Cantor-type regions there are new gaps at every stage of the approximation and the total measure of the spectrum goes to zero. In bandlike regions the wave functions are extended; in Cantor-type regions they are localized. Extended states correspond to continuous densities in the unit cell of the superspace symmetry group, whereas localized states correspond to discontinuous ones. In this respect the model seems to behave slightly different from the tight-binding model studied by other authors.

Aubry has found for a tight-binding model with sinusoidal modulation that all states are localized, if the modulation amplitude exceeds a critical value; otherwise they are extended. Sokoloff, using Anderson's locator method, found, for the same model, agreement with Aubry for modulation amplitudes larger than the critical value. For smaller values there is a mobility edge (for large modulation wave vector q) or a collection of narrow bands separated by gaps for small q. The type of localization studied by Aubry has a different nature, though. The superspace plot showed us that the localized states in the Kronig-Penney model correspond to nonanalytic behavior in the internal coordinate t, whereas in Aubry's case the wave function is nonanalytic in the space coordinate itself. Of course, this kind of behavior may also occur for the Kronig-Penney model, if the amplitude of the modulation function or alternatively the strength of the δ potentials is blown up.

For the Kronig-Penney model Azbel found a mobility edge between localized and extended states using semiclassical methods. Our investigation confirms this picture: There are both localized and extended states. However, this depends strongly on the modulation wave vector. So, although we did not investigate the spectrum as a function of the modulation amplitude, a metal-insulator transition is also possible in the case studied in the present paper, if the states at the Fermi level change their character with changing modulation wave vector (which can be induced by a change in temperature).

For the tight-binding model Aubry has shown that, in case the modulation function itself becomes nonanalytic, all states are localized. Actually, the system then behaves like a disordered one. For the modulated Kronig-Penney model we considered an analytic (sinusoidal) modulation function only, and the behavior is certainly different.

Contrary to what happens in amorphous solids in more than one dimension, where there exists a mobility edge which separates extended states in the center of the band from localized states at the band edges, the character of the states in the modulated Kronig-Penney model does not depend much on the wave vector k. Therefore, in our case localized and extended states may occur simultaneously, but they are separated by gaps. Recently, this behavior has also been observed in a tight-binding model with nonsinusoidal modulation.[33]

As has become clear from recent publications[13–22] one should be very careful in generalizing results for specific models or for particular values of the modulation wave vector. In particular unexpected things may happen if $q/2\pi$ is a so-called Liouville number.[13]

Bellissard *et al.*[17] have found an interesting relation between the tight-binding model in one dimension studied by Aubry[8] and the Kronig-Penney model with modulated strengths of the δ-function potentials. In this way they can use results for the former model to this Kronig-Penney problem. Like Aubry they find a metal-insulator transition in the latter at a critical value of the modulation ampli-

tude, in contrast to the transition found in the present paper for varying modulation wave vector.

We want to conclude with two remarks concerning common features of the Kronig-Penney model and the tight-binding model. Sokoloff has studied the dependence of the band structure of the tight-binding model on the phase of the modulation function.[10] He found that for bands of extended states the energy is nearly independent of the phase. In this respect, it should be mentioned that Butler and Brown also studied the tight-binding model.[34] They derived an explicit analytical expression for the dependence of the spectrum on the phase of the modulation function. This should be studied in more detail. For incommensurate modulation wave vectors the situation ought to be like this, because then the spectrum is the same regardless of the value of the phase, unless, as Aubry argued, an analyticity break in the wave functions occurs, through which the electrons become localized. Indeed, Sokoloff found that for localized states the band structure becomes phase dependent. For the Kronig-Penney model we found a similar behavior. The three lowest, extremely narrow bands for $q/2\pi=\frac{3}{50}$, for example, which correspond to nonlocalized states, are independent of phase, whereas the lowest subband for $q/2\pi=\frac{7}{53}$, whose width is comparable, varies considerably with phase.

Another interesting observation concerns the widths of the gaps. Zilberman has studied the tight-binding model, using the same WKB methods as Azbel, to establish the relation between the continued-fraction expansion of the modulation wave vector and the band structure.[31] Zilberman's analysis shows that the largest gaps are found at the edges of the band clusters. Towards the center of the clusters they diminish exponentially. This behavior is easily observable for small values of the modulation wave vector for which Zilberman's approach originally applied due to the nature of the WKB method (however, as we have mentioned before, Sokoloff has extended the analysis to arbitrary values of the modulation wave vector). Exactly the same behavior is found for the Kronig-Penney model.

ACKNOWLEDGMENTS

We wish to thank Professor A. G. M. Janner for many stimulating discussions on incommensurate crystal phases, Professor J. Sokoloff for drawing our attention to the work of Bellissard *et al.*, and Professor B. Simon, Professor J. Arron, and Professor J. Bellissard for sending us their papers prior to publication.

[1]R. E. Peierls, *Quantum Theory of Solids* (Clarendon, Oxford, 1955).
[2]H. Fröhlich, Proc. R. Soc. London 223, 296 (1954).
[3]J. Przystawa, in *Physics of Modern Materials* (International Atomic Energy Agency, Vienna, 1980), Vol. II, p. 213.
[4]P. M. de Wolff, Acta Crystallogr. Sec. A 30, 777 (1974).
[5]A. Janner and T. Janssen, Phys. Rev. B 15, 643 (1977).
[6]C. de Lange and T. Janssen, J. Phys. C 14, 5269 (1981).
[7]D. R. Hofstadter, Phys. Rev. B 14, 2239 (1976).
[8]S. Aubry, in *Bifurcation Phenomena in Mathematical Physics and Related Topics,* edited by C. Bardos and D. Bessis (Reidel, Dordrecht, 1980), p. 163.
[9]J. B. Sokoloff, Phys. Rev. B 22, 5823 (1980).
[10]J. B. Sokoloff, Phys. Rev. B 23, 6422 (1981).
[11]T. Janssen and A. Janner, in *Symmetries and Broken Symmetries in Condensed Matter Physics,* edited by N. Boccara (Institut pour le Développement de la Science, l'Education et la Technologie, Paris, 1981), p. 211.
[12]E. I. Dinaburg and Ya. G. Sinai, Funkt. Anal. Pril. 9, 8 (1975) [Funct. Anal. Appl. 9, 279 (1975)].
[13]B. Simon, Adv. Appl. Math. (in press).
[14]J. Bellissard, B. Simon, J. Funct. Anal. 48, 408 (1982).
[15]J. Avron, B. Simon, Commun. Math. Phys. 82, 101 (1981).
[16]J. Bellissard and D. Testard (in press).
[17]J. Bellissard, A. Formoso, R. Lima, and D. Testard, Phys. Rev. B 26, 3024 (1982).
[18]J. Bellissard and D. Testard (unpublished).
[19]J. Bellissard and E. Scoppola, Commun. Math. Phys. 85, 301 (1982).
[20]J. Bellissard, R. Lima, and D. Testard, Comm. Math. Phys. (in press).
[21]J. Bellissard, D. Bessis, and P. Moussa (unpublished).
[22]J. Bellissard, R. Lima, and E. Scoppola, Comm. Math. Phys. (unpublished).
[23]T. Janssen, J. Phys. C 12, 5381 (1979).
[24]M. Ya. Azbel, Phys. Rev. Lett. 43, 1954 (1979).
[25]M. Toda, *Theory of Nonlinear Lattices* (Springer, Berlin, 1981).
[26]M. Ya. Azbel, Zh. Eksp. Teor. Fiz. 46, 929 (1964) [Sov. Phys.—JETP 19, 634 (1964)].
[27]J. B. Sokoloff, Phys. Rev. B 23, 2039 (1971).
[28]T. Janssen and C. de Lange, J. Phys. (Paris) Colloq. C6 42, 737 (1981).
[29]J. B. Sokoloff, Solid State Commun. 40, 633 (1981).
[30]R. E. Borland, Proc. R. Soc. London Ser. A 274, 529 (1963).
[31]G. E. Zilberman, Zh. Eksp. Teor. Fiz. 32, 296 (1957) [Sov. Phys.—JETP 5, 208 (1957)].
[32]B. B. Mandelbrot, *Fractals: Form, Chance and Dimension* (Freeman, San Francisco, 1977).
[33]C. M. Soukoulis and E. N. Economou, Phys. Rev. Lett. 48, 1043 (1982).
[34]F. A. Butler and E. Brown, Phys. Rev. 166, 630 (1968).